No evidence of sexual conflict for a novel sperm-derived seminal fluid protein in *Caenorhabditis* nematodes

Short Title: NSPF proteins promote fitness without sexual conflict

Katja R. Kasimatis[1]*, Christine Rehaluk[1], Locke Rowe[1], and Asher D. Cutter[1]*

[1]Department of Ecology and Evolutionary Biology, University of Toronto, Toronto, Ontario, Canada

*Corresponding authors: k.kasimatis@utoronto.ca (KRK) and asher.cutter@utoronto.ca (ADC)

ABSTRACT

Post-insemination molecular interactions involving sperm are an ideal system for linking genotype, phenotype, and fitness. Nematode sperm contain subcellular vesicles known as membranous organelles (MOs) that fuse with the cell membrane upon sperm activation to release their soluble contents into the extracellular space. The second most abundant protein group in the MOs is the conserved Nematode-Specific Peptide family, group F (NSPF) gene family.

We hypothesize that these proteins contribute to seminal fluid upon MO fusion and are part of post-insemination reproductive tract dynamics. We used experimental evolution to compete the wildtype allele against a deletion allele in 10 replicate populations. We calculated a significant mean selective disadvantage of 0.1% for the deletion allele, which indicated that the NSPF genes are an evolutionarily important component of male reproductive success. This conclusion was reinforced by qualitative trends from lower powered single-generation male fertility assays. We then characterized the functional location of NSPF proteins during fertilization using whole-worm immunostaining of a His-tagged *nspf-1* transgene. Throughout male development, we found that NSPF presence and abundance was correlated with reproductive maturity in males, localizing to the seminal vesicle during L4 and to the spicules throughout adulthood. We confirmed that NSPF proteins are transferred to females during mating and hypothesize that proteins adhere to the spicules during transfer. NSPF proteins localize to the vulva and uterus lumen when transferred to mated females and in unmated adult hermaphrodites. These results suggest that the uterine localization of the NSPF proteins is likely a functional property of both male-derived sperm and self-sperm and not simply incidental to the point of transfer during mating. Our study demonstrates that nematodes use a novel mechanism for generating seminal fluid proteins and shows that the highly abundant NSPF proteins likely have a female-beneficial fitness effect.

INTRODUCTION

To understand the extent of adaptive evolution, we must link a phenotype with its underlying genetic basis and effect on fitness (Barrett and Hoekstra 2011). By connecting the layers of the genotype-phenotype-fitness map we gain insight on the mechanisms that drive adaptation (Lewontin 1974). Understanding these linkages will often demand an integrated, interdisciplinary experimental approach, which is necessarily challenging. Post-insemination reproductive interactions, however, offer an ideal stage of the lifecycle for mapping these relationships because their impact on reproductive fitness is direct, such that an adaptive advantage of one variant over another should lead to an increase in reproductive success. Additionally, the interactions involving cells, proteins, and small molecules simplifies the mapping of their genetic basis (McDonough et al. 2016). Despite these direct and simplified linkages, connecting reproductive genes with a clear, consistent phenotype and a reproducible, quantifiable effect on fitness has proved challenging.

Post-insemination reproduction studies have largely focused on interactions mediated by seminal fluid. Seminal fluid is a complex mixture of cells, proteins, and other small molecules that are transferred to the female along with sperm (Poiani 2006; Perry et al. 2013). As a whole, seminal fluid is critical for male and female fertility – sperm alone is not enough to ensure fertilization – and is implicated in complex behaviors, such as sperm competition, male-female signaling and conflict (Poiani 2006). Most functional work on these seminal fluid proteins comes from the study of dozens of *Drosophila* accessory gland proteins (Acps) (Chapman 2011). The genes underlying many of these Acps are characterized by their elevated evolutionary rate relative to non-reproductive proteins, indicating adaptive evolution (Begun et al. 2000; Swanson and Vacquier 2002; Clark et al. 2006; Wilburn and Swanson 2016). The complexity of seminal fluid proteins coupled with their rapid evolution and some evidence of harmful effects on females have led to the paradigm that these proteins are beneficial to male fitness but detrimental female fitness (Sirot et al. 2015). Perhaps the best studied Acp, Sex Peptide, has become a textbook example of post-insemination sexual conflict (Arnqvist and Rowe 2005; Hopkins and Perry 2022). However, this protein does not always fit the conflict paradigm it has come to represent (Hopkins and Perry 2022). In particular, molecular evolution analysis of Sex Peptide indicates molecular constraint, which is not consistent with evolution driven by sexual conflict (Cirera and Aguade 1997). Additionally, when individual components of fitness have been

quantified, environmental factors appear to impact when Sex Peptide is detrimental or even beneficial to female fitness (Hopkins and Perry 2022). These deeper analyses along with similar studies on other Acps (Wong and Rundle 2013) suggest that seminal fluid evolution is more nuanced than the sexual conflict narrative alone and indicate that employing new approaches and new taxa may provide a more precise and complete understanding of the complex roles and fitness effects of seminal fluid proteins.

Caenorhabditis nematodes offer a powerful model system for integrating across the layers of the genotype-phenotype-fitness landscape and are ideal for expanding our view on the extent of evolution by sexual conflict and for discovering new roles for seminal fluid proteins. First, the mating system differs across the genus, with *C. elegans* representing a lineage transition from obligate outcrossing to hermaphroditic self-fertilization (Baldi et al. 2009). Using the genetic tools developed in *C. elegans*, researchers can manipulate hermaphrodites to develop as pseudo-females that rely on males to reproduce, which allows direct comparison of the genetics and fitness effects between self-sperm and male-derived sperm to disentangle conflict and cooperation. Additionally, broader contrasts can be made among closely related species with different mating systems and therefore varying opportunities for sexual conflict (Ting et al. 2014; Yin et al. 2018). Second, the small size and rapid generation time of nematodes make them amenable to fitness assays within and across multiple generations. Multi-generation assays allow for detection and quantification of even small fitness effects. Finally, nematodes have unique amoeboid crawling sperm which can be visualized through the transparent cuticle, allowing for spectacular live visualization of sperm and seminal fluid dynamics inside of females or hermaphrodites (Smith and Stanfield 2011; Ting et al. 2014; Hansen et al. 2015; Yin et al. 2018). Very few seminal fluid proteins, however, have been identified and functionally examined in *Caenorhabditis* (Smith and Stanfield 2011; Yin et al. 2018). Thus, this system provides an underexploited opportunity for discovering new features of reproductive evolution to evaluate and, perhaps, that can challenge existing paradigms.

An intriguing component of nematode sperm cells are subcellular vesicles known as membranous organelles (MOs). In inactive spermatids, MOs are located around the periphery of the cell (Ellis and Stanfield 2014). Upon ejaculation, spermatids are released from the seminal vesicle and undergo activation as they pass through the vas deferens. During activation, MOs fuse with the cell membrane and create cup-like structures as well as releasing their soluble

protein contents into the extracellular space (Ellis and Stanfield 2014). No accessory gland-like tissues have been identified in *Caenorhabditis* and the source – as well as contents – of seminal fluid are unknown. Consequently, we hypothesize that these MO fusions provide a novel contribution to the seminal fluid proteome. Characterization of the MO proteome identified the Nematode-Specific Peptide family, group F (NSPF) as the second most abundant set of proteins in the MO (Kasimatis et al. 2018). We showed that the NSPF genes are conserved in both sequence identity and synteny across the genus (Kasimatis et al. 2018). Transcriptomic data support the molecular evolution analyses by capturing NSPF expression in *C. elegans* males along with NSPF ortholog expression in *C. remanei* males (Albritton et al. 2014). Interestingly, transcriptomic data also identify expression in *C. elegans* hermaphrodites but not *C. briggsae* hermaphrodites, suggesting that this gene family has been conserved in at least some self-sperm pathways (Albritton et al. 2014).

Here we investigate the function of the NSPF gene family in fertilization by interconnecting the layers of the genotype-phenotype-fitness landscape. We estimate the contribution of the NSPF genes to reproductive fitness using a combination of within generation fertility assays and 20 generations of experimental evolution. We then use immunostaining to identify the functional regions that NSPF proteins are associated with in males and females/hermaphrodites. Our results indicate that the NSPF proteins are a novel component of seminal fluid with a small-magnitude net fitness benefit and imply that even a highly abundant and conserved seminal fluid protein can have a subtle function.

RESULTS

Deletion of the NSPF genes decreases male fitness

Previous experiments on young adult male fertility showed no significant difference in total fecundity between wildtype males and males with all three copies of the NSPF genes deleted (i.e., deletion allele) (Fig. S1A) (Kasimatis et al. 2018). Using old males (day 5 of adulthood), we repeated these non-competitive, total fecundity assays to determine whether NSPF proteins improved male sperm fertilization ability in a phase of the life cycle when male fertility is declining overall. Although the mean fecundity of old males with the deletion allele trended lower than wildtype males (x_{del} = 459; x_{wt} = 481.9), the effect was not significant (p = 0.85; Fig. S1A), and thus there is no indication of a strong cost to females. This nominal decrease in

fecundity of males with the deletion allele was similar to what was previously seen with young adult males under a competitive male setting, suggesting that NSPF function is potentially age-independent (Kasimatis et al. 2018 Fig. S1B). However, given the experiment size and high reproductive variance, a difference between genotypes of 71% would be required to achieve 80% power to detect a significant difference. Thus, within-generation assays likely are not sufficiently sensitive to capture the nuanced fitness effects suggested by the trend means, despite the high abundance of these proteins.

We turned to experimental evolution to overcome these power limitations of within-generation experimental design. Specifically, we competed the wildtype allele against the deletion allele in an obligate outcrossing *C. elegans* population by evolving ten replicate populations of 1,000 individuals from a base population that was heterozygous at the NSPF locus in an otherwise homogeneous genetic background. After 20 generations, we documented a significant overall decrease in the frequency of the deletion allele across replicates (Model 1: z-value = 3.3, p = 0.001; Model 2: z-value = 2.3, p = 0.02). Additionally, the change in frequency exceeded that expected by neutral processes alone in seven of the ten replicates (Fig. 1). These results support the within generation fecundity trends and indicate a direct net fitness cost when the NSPF genes are removed, such that the wildtype allele confers an approximately 0.1% fitness advantage over the deletion allele (Model 1: $s = 0.001$; Model 2: $s = 0.0008$). Together, the favoring of the wildtype allele coupled with the fecundity do not provide evidence of a cost of the NSPF proteins to mating females. Rather, they provide a net fitness effect that is consistent with being beneficial to one or both sexes.

NSPF proteins localize to the spicules in adult males

We characterized the functional location of NSPF proteins during fertilization using whole-worm immunostaining of a His-tagged *nspf-1* transgene re-inserted into the deletion allele background (PX814). We scored the presence the fluorescent antibody bound to NSPF-1::6xHis in six anatomical regions: head, distal gonad, proximal gonad, vas deferens, cloaca, and tail (Fig. 2A). Throughout male development, we found that NSPF presence and abundance was correlated with male reproductive maturity (Fig. 2B; Fig S2). During larval stage 3 (L3), the gonad is still developing and no staining was present, which supports our previous finding that NSPF production is linked with sperm production (File S1). Sperm production begins during the L4 stage and correspondingly L4 males had staining in both the distal (n = 17 of 126) and proximal

gonad (n = 1 of 126; Fig. 3A). Interestingly, 43% of males had staining in the tail region (n = 55 of 126) specifically overlapping with the spicules. These patterns are significantly different from control males ($\chi^2 = 175.5$, df = 3, $p < 0.0001$), of which only one male showed non-specific staining along the cuticle in the proximal gonad region (Fig. 3B).

In adult males, NSPF proteins localized solely to the spicules (Fig. 3C). Abundance appeared highest on days 1 and 2 of adulthood with 100% of males (n = 100 and 150, respectively) showing staining in the tail region (Fig. 2B). Again, these patterns were significantly different from the off-target staining or spicule auto-fluorescence observed in control males during day 1 (n = 13 of 99 stained; $\chi^2 = 149.5$, df = 1, $p < 0.0001$) and day 2 (n = 45 of 150 stained; $\chi^2 = 158.5$, df = 1, $p < 0.0001$) of adulthood (Fig. 3D). Older males, however, had a decreased signal of NSPF proteins (n = 59 of 106), though still significantly different from control males ($\chi^2 = 39.4$, df = 1, $p < 0.0001$). This pattern of protein abundance across development suggests that NSPF production is tightly correlated with spermatogenesis and peak reproductive output and mating activity during early adulthood.

Males transfer NSPF proteins to the female uterus during mating

To test our hypothesis that NSPF proteins form a constituent of seminal fluid, we examined whether males transferred NSPF proteins during mating. Specifically, control pseudo-females (JK574) were mated with His-tagged males (VX300) for 24 hours. Of the pseudo-females without eggs in utero, 38% (n = 8 of 21) had a clear signal of staining around the vulva and in the uterine space (Fig. 4A). This signal was significantly different from that of control females mated to control males ($\chi^2 = 9.7$, df = 2, $p = 0.008$; Fig. 4B). Only 12% (n = 15 of 129) of pseudo-females with eggs in utero showed a clear signal of staining, which was not significantly different from pseudo-females mated to control males ($\chi^2 = 0.53$, df = 1, $p = 0.47$). However, in these females the NSPF proteins appear to be in the uterus lumen, which suggests that eggs may mask the fluorescent signal (Fig. 4C). These results indicate that males transfer NSPF proteins during ejaculation and support our hypothesis that MOs contribute proteins to seminal fluid.

NSPF proteins localize to the uterus of unmated hermaphrodites

To determine whether self-sperm NSPF patterns differed from male-derived sperm patterns, we characterized NSPF localization in His-tagged hermaphrodites (VX300) raised in the presence of males throughout development. Again, L3 individuals showed no signal of staining (File S1). L4

hermaphrodites, however, had little to no staining and did not significantly differ from control females ($p = 1$; Fig. 2C) despite mRNA expression of *nspf-1* during this developmental stage (Harris et al. 2019). Adult hermaphrodites all showed the same vulva and uterus localization pattern of staining as observed in mated, control females (Fig. 2C; Fig. S2). On days 1 and 2 of adulthood 54% (n = 54 of 100) and 41% (n = 61 of 150) of hermaphrodites, respectively, showed staining, which was significantly more than control females (Day 1: $\chi^2 = 49.9$, df = 1, $p < 0.0001$; Day 2: $\chi^2 = 22.6$, df = 1, $p < 0.0001$). On day 8 of adulthood, 67% (n = 90 of 134) of hermaphrodites showed the same significant staining pattern ($\chi^2 = 147.2$, df = 6, $p < 0.0001$; Fig. 2C). Since self-sperm is depleted this late in adulthood (Hirsh et al. 1976), these data further support the male transfer of NSPF proteins to the uterus. Across all developmental time points, there was an unexpected absence of signal in the spermathecae, likely due to experimental constraints.

To distinguish whether the early adulthood signal of NSPF staining was caused by self-fertilization or mating, we examined a male-less population of His-tagged hermaphrodites on day 1 of adulthood prior to the start of egg laying. If the NSPF proteins were costly to female reproduction, then we would expect self-sperm derived NSPF to be lost or significantly reduced. We found that 59% (n = 59 of 100) of hermaphrodites showed the same vulva and uterus pattern of staining (Fig. 4D) despite no opportunity for male transfer of NSPF proteins. This frequency was not significantly different from the number of day 1 hermaphrodites raised in the presence of males ($p = 0.57$). These results suggest that the uterine localization of the NSPF proteins – whether secreted by self-sperm or male sperm – likely reflects their site of activity and not simply a byproduct of the point of transfer during mating. Moreover, they reinforce the benefit of NSPF proteins to reproductive fitness and imply that this benefit is directed toward female reproduction.

DISCUSSION

Seminal fluid is a complex bioactive mixture whose components are implicated in a variety of reproductive, behavioral and physiological functions and thus likely evolves under multiple selective pressures. By linking the genes creating seminal fluid proteins with their evolutionary history, effect on fitness, and phenotypic contribution we can understand the evolutionary forces driving seminal fluid evolution through its impacts on reproductive function. We took an

integrative approach to connect the highly abundant MO NSPF proteins across the genotype, phenotype, fitness landscape. We confirmed that the NSPF genes are indeed a component of seminal fluid that is transferred to females, which demonstrates that MO fusion provides a novel source of seminal fluid proteins. Moreover, the localization of NSPF proteins differ from that of mRNA transcripts, highlighting the nested layers between genotype space and phenotype space that can often be overlooked. Finally, we quantified the small, but significant contribution made to reproductive fitness by the presence of NSPF proteins, suggestive of a fitness benefit potentially to females. Together this work demonstrates the power of *Caenorhabditis* to disentangle beneficial versus antagonistic effects of seminal fluid proteins and to expand our perspective of seminal fluid protein function.

The manipulable hermaphroditic mating system of *C. elegans*, relative to study systems like *Drosophila*, offers a novel means of distinguishing sexual conflict from sexual cooperation between male-derived sperm and self-sperm interactions (Schärer et al. 2015). We capitalized on this advantage to show that NSPF production is not only retained during the lineage transition to self-fertilization, but that the proteins localize to the same uterus region in unmated hermaphrodites as in mated females (Fig. 4). This pattern is congruent with the conserved molecular evolution of the *nspf* gene sequences and implies that the function of the sperm-dependent NSPF proteins within the uterus is mating-independent. Importantly, the conserved expression in hermaphrodites indicates that these proteins are not involved in sexual conflict, as there would be strong selection favoring their loss (Yin et al. 2018). Instead, these genes appear beneficial to female function, as supported by fitness assays. In particular, if NSPF genes provided an advantage to males to the detriment of females, we would expect females mated with deletion-allele males to trend toward higher reproductive success than females mated with wildtype males. However, our assay and previous assays support the opposite of such a scenario, suggesting NSPF promotes sexually-concordant reproductive fitness, as shown more convincingly during experimental evolution.

A common challenge in evolutionary biology is to detect the fitness effects of variants at a single gene (Barrett and Hoekstra 2011). Our experimental evolution design to compete the wildtype and deletion alleles in a highly-replicated fashion allowed us to compound small effect sizes over tens of generations. The nematode model system allows for this approach to be carried out at a larger scale and over a longer time periods than similar studies (Wong and Rundle 2013),

which, when coupled with genomics, provides greater power to detect small or fluctuating selection coefficients. The overall trend across replicates was a decrease in the frequency of the deletion allele beyond the neutral expectation (Fig. 2). The estimated selection coefficient, despite being small, would be powerful enough to prevent *nspf* gene loss over time in nature. The frequency of the deletion allele did not continually decrease in every replicate at each sampling time point, however, which likely reflected a combination of variance and stochasticity during mating along with sampling error and the relatively small selection coefficient. The fluctuation of the deletion allele could also reflect the environment conditions in the lab which do not perfectly replicate nature, where the NSPF proteins may provide a greater or more consistent benefit in populations with larger effective sizes. This approach of allelic competition in experimental evolution (Gray & Cutter 2014; Teotonio et al. 2017) may represent a promising avenue for future seminal fluid protein studies, and for genetic variants of other phenotypes, where small fitness effect sizes have proved challenging to characterize.

The localization of NSPF protein to the spicule (Fig. 3) and uterus (Fig. 4) was unexpected given that the NSPFs were previously characterized as being associated with sperm MOs (Kasimatis et al. 2018) and that mRNA expression data indicated that all three *nspf* genes are expressed in the gonad only (Kruse et al. 2016). One potential reason for the non-overlapping localization patterns could be an artifact of our experimental set-up. Specifically, whole worm immunostaining may lack the sensitivity to visualize staining within small sperm subcellular structures. Our approach did, however, identify additional regions of localization that may result from the anatomical difference in the location of inactivated versus activated sperm. The activation process occurs as sperm pass from a male to a female/hermaphrodite while the spicules are everted in the vulva, thus creating a direct link between MO fusion and the spicules. This overlap in timing, however, does not explain the spicule signal seen in L4 males, which warrants further work. In hermaphrodites, the parsimonious hypothesis is that NSPF proteins passively diffuse from the spermathecae, where activated sperm reside, to the uterus. The location of NSPF proteins within the uterus is similar to other proteins that males transfer, which originate in newly identified extracellular vesicles (Nikonorova et al. 2022). While the NSPFs do not appear in these vesicles, it is possible that this alternative vesicle type also contributes to seminal fluid proteins, supporting our finding that nematodes employ a distinct mechanism for secreting seminal fluid proteins than either mammals or *Drosophila* (McGraw et al. 2015).

Our data motivate multiple hypotheses for future testing to narrow down the specific beneficial function of the NSPF proteins. First, the NSPF proteins could interact with a male-female signaling network that promotes egg laying. While the interacting partner for NSPF proteins remains unknown, it is possible that NSPFs bind to muscle proteins that form the uterus walls and are involved in egg laying behavior. Under this hypothesis, localization to the spicules is puzzling. However, previous work has shown the females pressurize the gonad to push some of the ejaculate mass and spicules out of the vulva (Barker 1994). This process could create a residue on the spicule cuticle as a byproduct, though we cannot rule out a functional relationship between the NSPF proteins and spicule cuticle.

Alternatively, the NSPF proteins could impact the uterine environment. Specifically, seminal fluid of some species contains anti-microbial factors (Samakovlis et al. 1991; Gao and Zhu 2016). Given the density of protein right above the vulva, one hypothesis is that the NSPF proteins play an anti-microbial role to protect the uterus from bacterial infection. Previous work has shown that the uterus is exposed to pathogenic infection from the external environment during mating and egg laying (Muir and Tan 2008). The male spicules are presumably also exposed during eversion, and thus any anti-microbial activity of the NSPF residue on the spicules might serve to prevent bacterial infection when the spicules retract. Biochemically, the alpha-helix structure of NSPF proteins lends plausibility to this hypothesis, as such secondary structures can confer generic bacterial lysing properties (Huan et al. 2020). Future work testing the fitness effects of the NSPF deletion allele in worms raised in more pathogenic bacteria is warranted.

Our work demonstrates the complex but subtle dynamics of seminal fluid proteins uncovered when using integrative approaches. The NSPF seminal fluid proteins, in particular, appear to exhibit sexually-concordant rather than sexually-antagonistic fitness effects. We also showed how *Caenorhabditis* nematodes are an excellent system for expanding our knowledge of post-insemination interactions not only for their technical benefits, but also for their novel sperm components and potential for making mating system contrasts. Connecting the layers of the genotype-phenotype-fitness map for seminal fluid proteins will help us uncover the genetics of fertility and the evolution of reproductive success.

MATERIALS AND METHODS

Molecular biology

To create a tagged *nspf-1* gene, guides targeting the sequence in the same intergenic region utilized by the ttTi5650 MosSCI site have previously been described (Dickinson et al. 2015) and inserted into pDD162 (Addgene #47549) to make plasmid pMS4. The repair template plasmid (pKK4) was assembled using the NEBuild HiFi Kit (NEB) from a combination of a restriction digest fragment and a synthetic gBlock Gene Fragment (IDT). The gBlock included the 647 base pairs upstream of *nspf-1* as the promoter region, the *nspf-1* coding sequence with six histidines added before the stop codon, and the *tbb-2* 3' UTR. The plasmid was purified using the GeneJET Plasmid Miniprep Kit (Thermo Scientific) and assembly junctions were verified by Sanger sequencing. A complete list of primers can be found in Table S1.

Strain generation

All strains used in this study are listed in Table S2. The NSPF genes were previously deleted using CRISPR/Cas9 to create strain PX814 (fxDf1 (II: 2,484,339 - 2,487,244)) (Kasimatis et al. 2018). To generate an obligate outcrossing deletion strain, JK574 (*fog-2*(q71) V) was crossed with PX814 and then backcrossed 5 times with JK574 to create the obligate outcrossing, deletion strain VX194. The deletion region was verified by Sanger sequencing.

Insertion of the His-tagged *nspf-1* transgene was done by CRISPR/Cas9 using standard methods (Dickinson et al. 2015). Briefly, a mixture of 10ng/µL repair template plasmid, 50ng/µL plasmid encoding CAS9 and the guide RNA, and 2.5ng/µL pZCS16 was injected into the gonad of young adult hermaphrodites from PX814. Hygromycin B (brand) was added to the injection plates at a final concentration of 250µg/mL three days after injection and hygromycin resistance (HygR) was used as a selectable event. Worms were kept at 25ºC for the first five days immediately following injections and then transferred for 20ºC for subsequent generations. Successful insertion was confirmed by PCR (Table S1) and Sanger sequencing. Worms were then backcrossed five times to PX814 to create the final strain VX300 (*nspf-1*p::*nspf-1*::6xHis::*tbb-2* 3' UTR + loxP). We tagged the N-terminus of *nspf-1* since these proteins are predicted signaling peptides (Kasimatis et al. 2018) and, thus, the N-terminus is likely included in the mature peptide.

Fertility Assays

We assayed the overall reproductive success of VX194 deletion males late in adulthood. We isolated virgin deletion males on day 1 of adulthood. On day 5 adulthood, single males were mated with three wildtype, virgin females (strain JK574) for 24 hours. As a control, wildtype males (strain JK574) were mated to wildtype females following the same timing and male to female ratio. Matings were conducted on small NGM-agar plates (35 mm diameter) seeded with 10µL OP50 *Escherichia coli*. After 24 hours, each male was removed and the females were transferred to a new small plate to continue laying eggs. Females were transferred to new plates every 24 hours until progeny production ceased. The total number of progeny was counted as a measure of each male's reproductive success (File S2). Fertility data were analyzed using R (R Core Team 2020), with the significance of non-competitive reproductive success evaluated using Welch's Two Sample t-test and an analysis of the power of the comparison computed. Previous fecundity data were replotted using the data available in Kasimatis et al. (2018) Additional File 9.

Experimental evolution design and worm culture

To create a base population, reciprocal crosses of virgin females and males from strains JK574 and VX194 were performed. The F1 heterozygous progeny were divided into 10 replicate populations of 500 worms with equal numbers of each sex to start the first generation. After generation one, populations were expanded to a census size of N = 1,000 worms per replicate and evolved for 20 generations. To start each generation, age synchronized larval stage 1 (L1) worms were plated onto four 10 cm NGM-agar plates seeded with OP50 *E. coli* at 20ºC with a density of 250 worms per plate (Brenner 1974; Kenyon 1988). Worms were left to mate for the first five days of adulthood before eggs were once again collected on day six to synchronize for the next generation. During this mating time, worms within each replicate were pooled and redistributed to fresh NGM-agar plates twice to ensure they never starved. A subset of worms from all replicates was frozen every five generations for future experiments. At generation eight all worms were frozen and the experiment paused for five months due to COVID-19 lockdown restrictions.

Amplicon sequencing and read calling

We performed amplicon sequencing on pooled samples of 500-800 L1 worms from experimental evolution generations 11 and 20. Two control samples were generated, each with approximately 700 worms: 1) F1 heterozygous progeny generated by crossing strains JK574 and VX194, and 2) pooled worms generated by mixing an equal number of JK574 and VX194 worms and sampling from this pool. The wildtype allele was amplified using forward primer (5' to 3') TGCAATGGATTTCTGGTGATAAC and reverse primer (5' to 3') TCTGGCAGTAGGAAAGTGAG, yielding a product of size 230 base pairs. The deletion allele was amplified using forward primer (5' to 3') AGGATAAGAGAGACCCAGAC and reverse primer (5' to 3') TCTGGCAGTAGGAAAGTGAG, yielding a product of size 275 base pairs. PCR products were generated using the OneTaq Quick-Load 2x PCR Master Mix with Standard Buffer (NEB) in accordance with manufacturer instructions with *C. elegans* genomic DNA. PCR products were purified using QIAquick PCR Purification kit (Qiagen) and normalized to 20ng/uL. Products were sequenced using GENEWIZ Amplicon-EZ services.

Reads for each sample were filtered using bioawk (https://github.com/lh3/bioawk) to exclude reads <50 base pairs in length and with a mean quality score <30. Reads in each sample >230 base pairs in length were then blasted to the deletion reference sequence and retained if the blast score was significant. All remaining reads were then blasted to the unique reference sequence for both the wildtype (bases 1-102) and deletion (bases 1-147) alleles (File S3). A read was called as a wildtype or deletion allele based on the best E-value and bit score. Final counts ranged from 89,721 to 132,685 reads per sample.

Estimating selection

Read data were analyzed using the R statistical language v4.0.0 (R Core Team 2020). Read counts across all time points were fit using a generalized linear mixed model with a binomial logistic distribution: glm((WT_{count}, DEL_{count}) ~ time). We fit two different linear models to account for biases during PCR amplification as suggested by the frequency of each allele in the control samples (i.e., 73% wildtype and 27% deletion). Model 1 assumed the frequency of each allele to be 50% (i.e., 500 copies of the wildtype allele and 500 copies of the deletion allele for a heterozygous population of N = 500), since all worms were heterozygous at the start of the experiment. Model 2 used only the allele frequencies estimated from the amplicon sequencing at generations 11 and 20. While we report the results of both models, Model 2 provides a better fit

($AIC_{Model\ 1}$ = 146,842; $AIC_{Model\ 2}$ = 146,670) and represents a more conservative estimate of selection.

The neutral expectation was determined by simulating in R allele frequency dynamics at a single locus in a population subject to genetic drift and random mating. We simulated 100 populations of 1,000 individuals. In the first generation, all individuals were heterozygotes. The genotype frequencies of females and males were multiplied to give a matrix of the relative frequencies of the possible random mating pairs. Mating pairs were then randomly sampled from this distribution to generate offspring to start the next generation.

Whole-worm immunohistochemistry

Worms were formaldehyde-fixed and stained following a modified version of the Ruvkun and Finney protocol (WormAtlas). Briefly, worms cultured at 20ºC on 10cm NGM-agar plates containing 100ng/mL carbenicillin and seeded with formaldehyde killed *E. coli* OP50 (following Rogers et al. 2006). At each developmental stage used, populations of at least 1,000 worms were fixed in a 1% formaldehyde solution and flash frozen in dry ice with ethanol. Incorrect antibody binding was blocked using solution of: 0.3M glycine, 10mM imidazole, 1% BSA, 0.5% skim milk, and 0.25% Triton-X-100 in PBS. Worms were stained for 1 hour at room temperature using a 1/4000 dilution of Recombinant Alex Fluor 488 Anti-6x His Tag antibody (Abcam #ab237336) and co-stained with DAPI. The complete method along with buffer recipes can be found in File S4.

To examine the localization of *nspf-1* in males and hermaphrodites across development, VX300 male-rich populations (~40% males) were age synchronized by bleaching (Kenyon 1988) and then formaldehyde-fixed during: L3 (28 hours post-L1), L4 (40 hours post-L1), day 1 of adulthood (46 hours post-L1), day 2 of adulthood (70 hours post- L1), and day 8 of adulthood (190 hours post-L1). As a control, JK574 males and pseudo-females were concurrently cultured and fixed at the same developmental stages. In our hands, worms developed more slowly and less synchronously on plates with dead OP50 than on live OP50. Thus, the exact time in development may be asynchronous between worms, but the developmental stages were accurate. At least 100 stained worms from each strain × sex × developmental stage were scored for the presence and location of fluorescence (File S1). The localization of fluorescence was characterized as occurring in one or more of the following regions: head, distal gonad, proximal

gonad (including the spermathecae or seminal vesicle), uterus/vas deferens, vulva/cloaca, or tail (Fig. 2A). Worms were categorized as "not stained" if no fluorescence was observed.

To determine whether or not males transfer NSPF-1 to females during mating, we crossed JK574 pseudo-females with VX300 males. Both strains were age-synchronized by bleaching followed by isolation of virgin pseudo-females (n = 400) and males (n = 150) during late L4 to 10cm NGM-agar plates containing 100ng/mL carbenicillin and seeded with formaldehyde-killed *E. coli* OP50 (n = 3 replicate plates). Worms were mated overnight and then formaldehyde-fixed and stained. One hundred pseudo-females were scored for the presence and location of fluorescence.

Count data for the presence of fluorescence were analyzed using a χ^2 test based on a contingency table of strain × presence of fluorescence for each sex and developmental stage separately. Specifically, we tested the null hypothesis of no difference between counts of stained individuals and counts of unstained individuals between the control (JK574) and His-tagged (VX300) strains. All analyses were conducted in R (R Core Team 2020).

Data accessibility

The oligonucleotides used in this study are available as Table S1. The immunostaining data are available in File S1 and the complete protocol is available in File S4. The fertility data are available in File S2. The raw amplicon data will be made publicly available at NCBI SRA upon publication. The processed amplicon reads are available in File S3. All scripts will be available via the Cutter Lab GitHub (https://github.com/cutterlab). Worm strains JK574 and VX300 are available from the *Caenorhabditis* Genetics Center. Strains PX814 and VX194 are available from the Cutter lab upon request.

Acknowledgements: We thank the Phillips lab for sharing plasmids pMS4 and pZCS16 and strain PX814. We thank Zachary Stevenson for transgenic advice, Jack Hu for immunostaining advice, and Stephen Banse, Eric Haig and the Cutter and Claycomb labs for their helpful discussion.

Funding: KRK is supported by a Natural Sciences and Engineering Research Council of Canada (NSERC) Banting Postdoctoral Fellowship. Funding to ADC was provided by the NSERC Discovery Grant Program. Funding to LR was provided by the NSERC Discovery Grant

Program and Canada Research Chairs Program. The funders had no role in study design, data collection and analysis, decision to publish, or preparation of the manuscript.

Author Contributions: KRK, ADC, and LR devised the project. KRK created strains VX194 and VX300. KRK performed the fecundity assay and experimental evolution. CR performed the immunostaining assays with assistance from KRK. KRK analyzed the data. KRK wrote the manuscript with the support of the other authors.

References

Albritton, S. E., A.-L. Kranz, P. Rao, M. Kramer, C. Dieterich, and S. Ercan. 2014. Sex-biased gene expression and evolution of the x chromosome in nematodes. Genetics 197:865–883.

Arnqvist, G., and L. Rowe. 2005. Sexual conflict. Princeton University Press, Princeton, NY.

Baldi, C., S. Cho, and R. E. Ellis. 2009. Mutations in two independent pathways are sufficient to create hermaphroditic nematodes. Science 326:1002–1005.

Barker, D. M. 1994. Copulatory plugs and paternity assurance in the nematode *Caenorhabditis elegans*. Animal Behaviour 48:147–156.

Barrett, R. D. H., and H. E. Hoekstra. 2011. Molecular spandrels: tests of adaptation at the genetic level. Nat Rev Genet 12:767–780.

Begun, D. J., P. Whitley, B. L. Todd, H. M. Waldrip-Dail, and A. G. Clark. 2000. Molecular population genetics of male accessory gland proteins in *Drosophila*. Genetics 156:1879–1888.

Brenner, S. 1974. The genetics of *Caenorhabditis elegans*. Genetics 77:71–94.

Chapman, T. 2011. Seminal fluid-mediated fitness traits in *Drosophila*. Heredity 87:511–521.

Cirera, S., and M. Aguade. 1997. Evolutionary history of the sex-peptide (Acp70A) gene region in *Drosophila melanogaster*. Genetics 147:189–197.

Clark, N. L., J. E. Aagaard, and W. J. Swanson. 2006. Evolution of reproductive proteins from animals and plants. Reproduction 131:11–22.

Dickinson, D. J., A. M. Pani, J. K. Heppert, C. D. Higgins, 2015. 2015. Streamlined genome engineering with a self-excising drug selection cassette. Genetics 200:1035–1049.

Ellis, R. E., and G. M. Stanfield. 2014. The regulation of spermatogenesis and sperm function in nematodes. Sem Cell Dev Biol 29:17–30.

Gao, B., and S. Zhu. 2016. The drosomycin multigene family: three-disulfide variants from *Drosophila takahashii* possess antibacterial activity. Nat Rev Genet 6:32175.

Hansen, J. M., D. R. Chavez, and G. M. Stanfield. 2015. COMP-1 promotes competitive advantage of nematode sperm. eLife 1–26.

Harris, T. W., V. Arnaboldi, S. Cain, J. Chan, W. J. Chen, J. *et al*. 2019. WormBase: a modern Model Organism Information Resource. Nucleic Acids Research 29:82.

Hopkins, B. R., and J. C. Perry. 2022. The evolution of sex peptide: sexual conflict, cooperation, and coevolution. Biol Rev 97:1426–1448.

Huan, Y., Q. Kong, H. Mou, and H. Yi. 2020. Antimicrobial peptides: classification, design, application and research progress in multiple fields. Front Microbiol 11:582779.

Kasimatis, K. R., M. J. Moerdyk-Schauwecker, N. Timmermeyer, and P. C. Phillips. 2018. Proteomic and evolutionary analyses of sperm activation identify uncharacterized genes in *Caenorhabditis* nematodes. BMC Genomics 19:593. BioMed Central.

Kenyon, C. 1988. The nematode *Caenorhabditis elegan*s. Science 240:1448–1453.

Kruse, F., J. P. Junker, A. van Oudenaarden, and J. Bakkers. 2016. Tomo-seq: A method to obtain genome-wide expression data with spatial resolution. Methods Cell Biol. 135:299–307.

Lewontin, R. C. 1974. The genetic basis of evolutionary change. Columbia University Press, New York.

McDonough, C. E., E. Whittington, S. Pitnick, and S. Dorus. 2016. Proteomics of reproductive systems: Towards a molecular understanding of postmating, prezygotic reproductive barriers. J. Proteomics 135:26–37.

McGraw, L. A., Suarez, S. S. and Wolfner, M. F. 2015. On a matter of seminal importance. Bioessays 37:142–147.

Muir, R. E., and M.-W. Tan. 2008. Virulence of *Leucobacter chromiireducens* subsp. solipictus to *Caenorhabditis elegans*: characterization of a novel host-pathogen interaction. Appl Environ Microbiol 74:4185–4198.

Nikonorova, I. A., J. Wang, A. L. Cope, P. E. Tilton, K. M. Power, J. D. Walsh, J. S. Akella, A. R. Krauchunas, P. Shah, and M. M. Barr. 2022. Isolation, profiling, and tracking of extracellular vesicle cargo in *Caenorhabditis elegans*. Curr. Biol. 32:1–13.

Perry, J. C., L. Sirot, and S. Wigby. 2013. The seminal symphony: how to compose an ejaculate. Trends Ecol Evol 28:414–422.

Poiani, A. 2006. Complexity of seminal fluid: a review. Behav Ecol Sociobiol 60:289–310.

R Core Team. 2020. R: A language and environment for statistical computing. Foundation for Statistical Computing, Vienna, Austria.

Rogers, A. B., K. S. Cormier, and J. G. Fox. 2006. Thiol-reactive compounds prevent

nonspecific antibody binding in immunohistochemistry. Laboratory Investigation 86:526–533.

Samakovlis, C., P. Kylsten, D. A. Kimbrell, A. Engström, and D. Hultmark. 1991. The andropin gene and its product, a male-specific antibacterial peptide in *Drosophila melanogaster*. The EMBO Journal 10:163–169. John Wiley & Sons, Ltd.

Schärer, L., T. Janicke, and S. A. Ramm. 2015. Sexual conflict in hermaphrodites. Cold Spring Harb Perspect Biol 7:a017673–25.

Sirot, L. K., A. Wong, T. Chapman, and M. F. Wolfner. 2015. Sexual conflict and seminal fluid proteins: a dynamic landscape of sexual interactions. Cold Spring Harb Perspect Biol 7:a017533.

Smith, J. R., and G. M. Stanfield. 2011. TRY-5 Is a Sperm-Activating Protease in Caenorhabditis elegans Seminal Fluid. PLoS Genetics 7:e1002375.

Swanson, W. J., and V. D. Vacquier. 2002. Reproductive protein evolution. Annu. Rev. Ecol. Syst. 33:161–179.

Ting, J. J., G. C. Woodruff, G. Leung, N.-R. Shin, A. D. Cutter, and E. S. Haag. 2014. Intense sperm-mediated sexual conflict promotes reproductive isolation in *Caenorhabditis* nematodes. PLoS Biol 12:e1001915.

Wilburn, D. B., and W. J. Swanson. 2016. From molecules to mating: Rapid evolution and biochemical studies of reproductive proteins. J. Proteomics 135:12–25.

Wong, A., and H. Rundle. 2013. Selection on the *Drosophila* seminal fluid protein Acp62F. Ecol Evol 3:1942–1950. John Wiley & Sons, Ltd.

Yin, D., E. M. Schwarz, C. G. Thomas, R. L. Felde, I. K. Science, 2017. 2018. Rapid genome shrinkage in a self-fertile nematode reveals sperm competition proteins. Science 359:55–61.

Figures

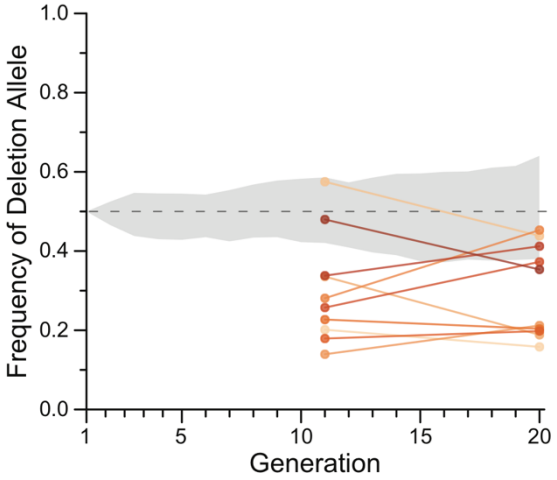

Figure 1. Changes in the frequency of the deletion allele over time estimated using amplicon sequencing data. All ten replicates started with 50% deletion allele (dashed line). The shaded gray region represents the expected allele frequency range under genetic drift and random mating estimated by simulation. There was a significant decrease in the frequency of the deletion allele over time (Model 1: $s = 0.001$, z-value = 3.3, $p < 0.001$; Model 2: $s = 0.0008$, z-value = 2.3, $p < 0.05$).

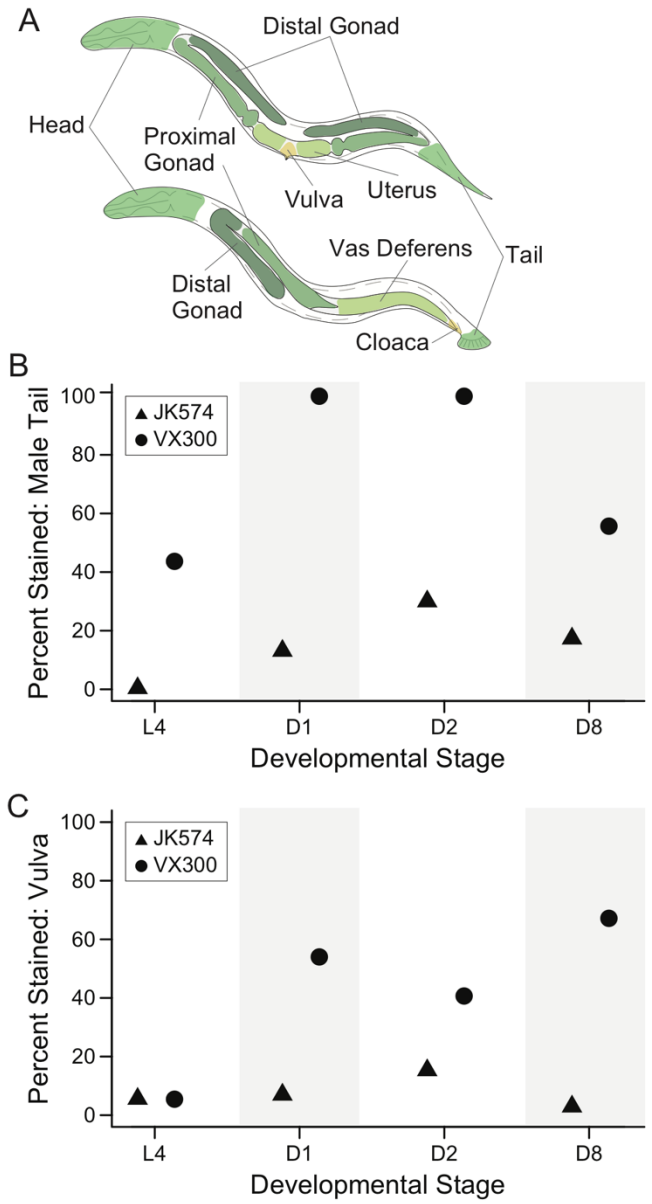

Figure 2. Quantification of antibody staining of 6x His-tagged NSPF-1. A) Diagram of the anatomical regions scored for presence of fluorescence in hermaphrodites/females and males. **B)** The percent of control males (JK574, triangle) and His-tagged males (VX300, circle) with fluorescence in the tail region during larval stage 4 (L4), day 1 of adulthood (D1), day 2 of adulthood (D2), and day 8 of adulthood (D8). **C)** The percent of control females (JK574, triangle) and His-tagged hermaphrodites (VX300, circle) with fluorescence in the vulva region during larval stage 4 (L4), day 1 of adulthood (D1), day 2 of adulthood (D2), and day 8 of adulthood (D8). Immunostaining counts across all anatomical regions is shown in Fig. S2.

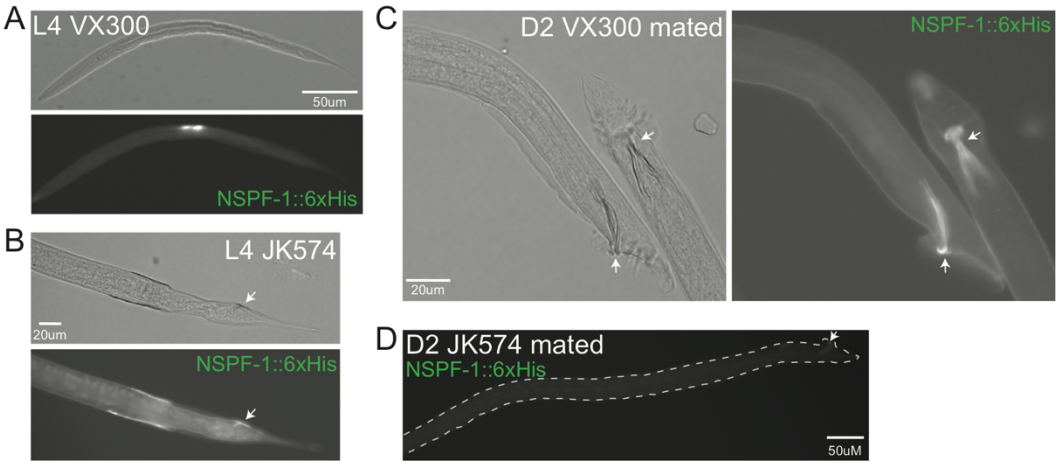

Figure 3. NSPF-1 localizes the spicules of adult males. A) Protein localized to the gonad of L4 His-tagged males. **B)** L4 control males showed off-target staining, especially in the cuticle, but not in the spicules. **C)** In adult His-tagged males, protein localized to the spicule structure in the male tail region. **D)** In adult control males, low levels of autofluorescence are detected in the spicules. However, the signal is markedly different than see in His-tagged males. In all images, the arrow points to the spicule.

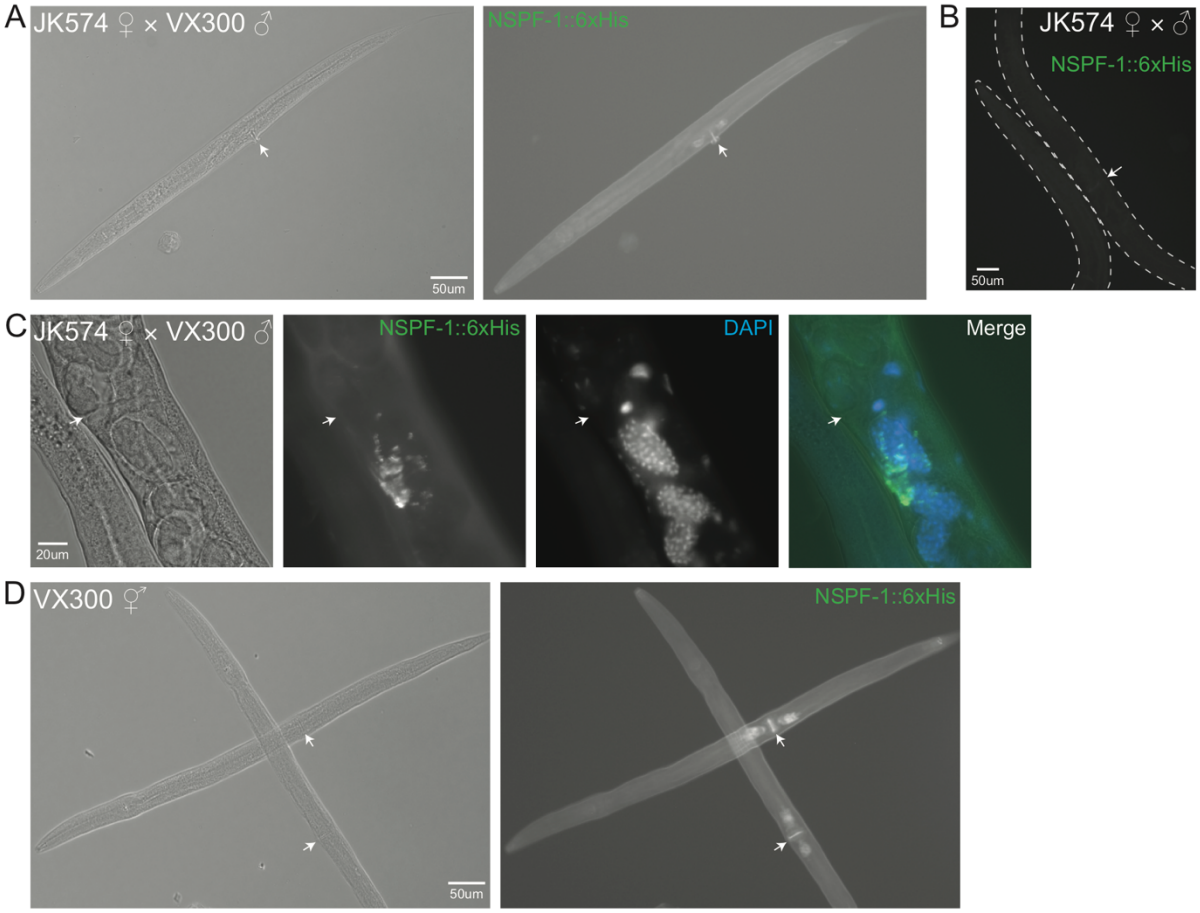

Figure 4. NSPF-1 localizes to the vulva and uterus of mated females and adult hermaphrodites. A) Control pseudo-females mated to His-tagged males showed evidence of protein localization in the vulva and uterus, especially when eggs were not yet present in the uterus. **B)** Control pseudo-females mated to control males showed no evidence of staining. **C)** Control pseudo-females mated with eggs present in the uterus after mating with His-tagged males also had protein present in the uterus, though the signal was not always clear. However, when present the proteins seemed to localize to the lumen and potentially along the surface of vulva muscle cells, as shown in the merged image. **C)** His-tagged adult hermaphrodites who had never been mated by a male showed the same protein localization in the uterus. In all images, the arrow points to the vulva.

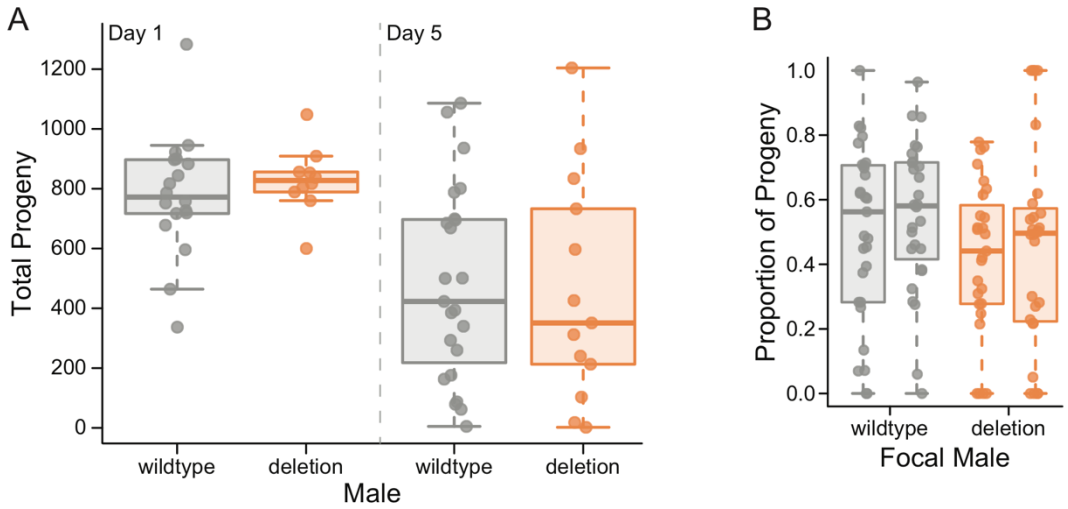

Fig S1. Single male fecundity assays. A) The total fecundity of wildtype males with the NSPF genes (gray) and deletion males with the NSPF genes removed (orange) at day 1 of adulthood and day 5 of adulthood. There was no significant difference in reproductive success between male types. Day 1 data were replotted from Kasimatis et al. (2018). **B)** The proportion of progeny coming from wildtype males (gray) or deletion males (orange) versus a wildtype competitor male. There was no significant difference in sperm competitive ability between male types (Kasimatis et al. 2018). Competitive fecundity success data were replotted from Kasimatis et al. (2018).

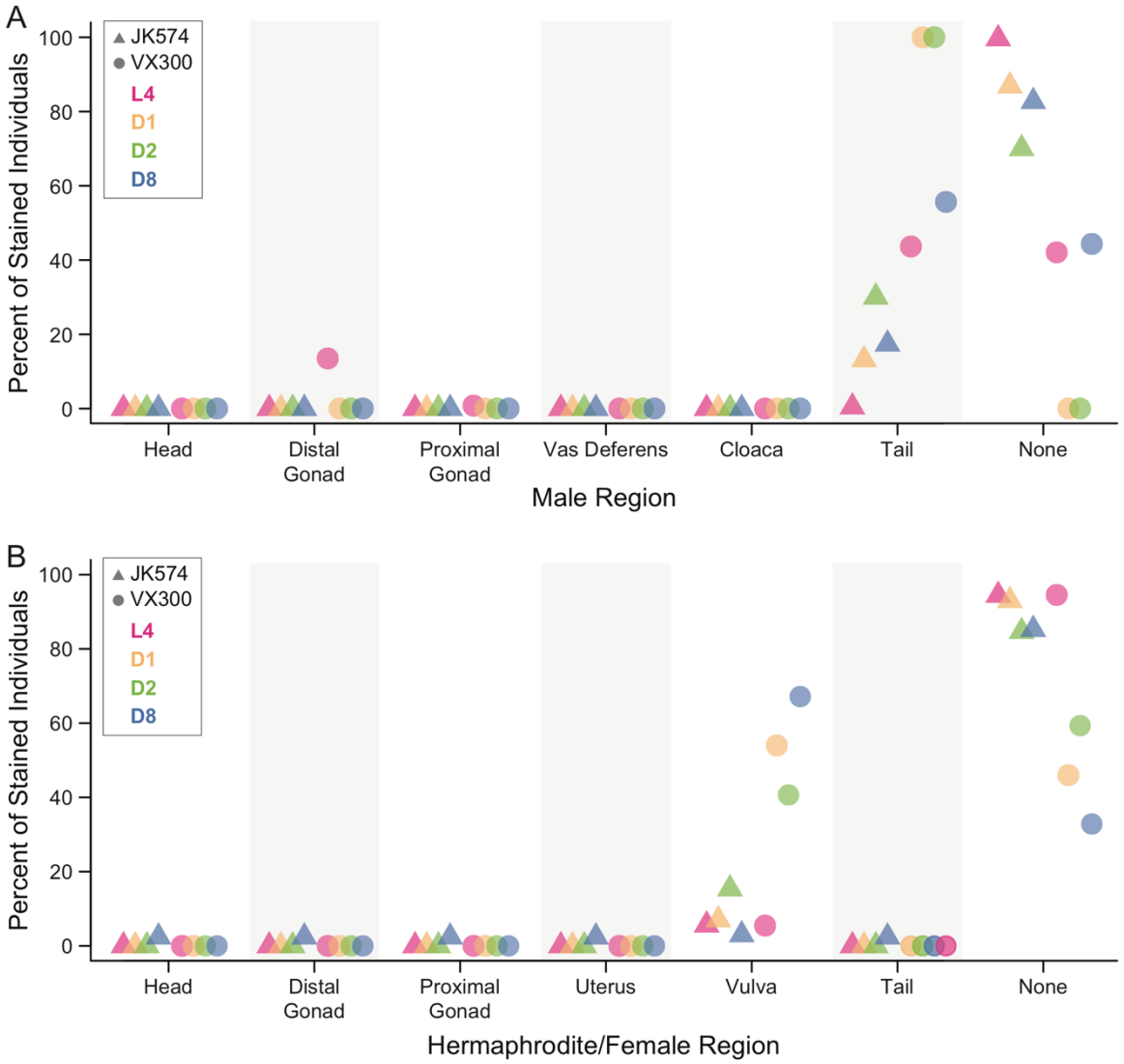

Fig S2. Immunostaining quantification development. A) Count data showing the percent of control males (JK574, triangle) and His-tagged males (VX300, circle) with fluorescence in each anatomical region during larval stage 4 (L4, orange), day 1 of adulthood (D1, green), day 2 of adulthood (D2, blue), and day 8 of adulthood (D8, pink). **C)** Count data showing the percent of control females (JK574, triangle) and His-tagged hermaphrodites (VX300, circle) with fluorescence in each anatomical region during larval stage 4 (L4, orange), day 1 of adulthood (D1, green), day 2 of adulthood (D2, blue), and day 8 of adulthood (D8, pink).

Supplemental Files

Table S1. Primers used in this study.

Table S2. Strains used in this study.

File S1. Immunostaining data.

File S2. Late life fecundity data.

File S3. Processed amplicon reads.

File S4. Complete immunostaining protocol and buffer recipes.